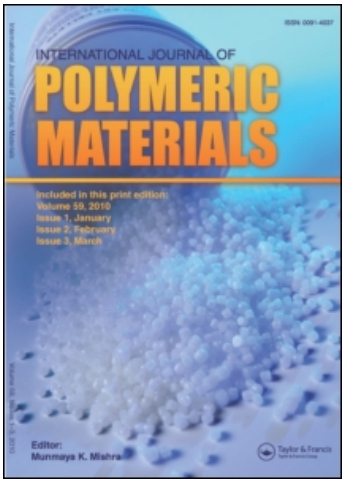

International Journal of Polymeric Materials
Publication details, including instructions for authors and subscription information:
http://www.informaworld.com/smpp/title~content=t713647664

Model of Nylon 6 Fibers Microstructure Microfibrillar Model or "Swiss-Cheese" Model?

V. Bukošek[ab]; D. C. Prevoršek[ab]
[a] Faculty for Natural Sciences, University of Ljubljana, Ljubljana, Slovenia [b] IJPM, Oregon, USA

To cite this Article Bukošek, V. and Prevoršek, D. C.(2000) 'Model of Nylon 6 Fibers Microstructure Microfibrillar Model or "Swiss-Cheese" Model?', International Journal of Polymeric Materials, 47: 4, 569 — 592
To link to this Article: DOI: 10.1080/00914030008031313
URL: http://dx.doi.org/10.1080/00914030008031313

Intern. J. Polymeric Mater., 2000, Vol. 47, pp. 569 – 592
Reprints available directly from the publisher
Photocopying permitted by license only

Model of Nylon 6 Fibers Microstructure Microfibrillar Model or "Swiss-Cheese" Model?

V. BUKOŠEK* and D. C. PREVORŠEK

University of Ljubljana, Faculty for Natural Sciences, Snežniška 5, Ljubljana, Slovenia, IJPM, Hood River, Montello Ave. 2, Oregon 97031-0021, USA

(Received 15 December 1998)

The microfibrillar morphological structure of aliphatic polyamide fibers has been consistently presented by the three phase microfibrillar model proposed by Prevoršek and not by the two phase microfibrillar model proposed by Peterlin. A widely spread opinion is that the 3-phase or "Swiss-cheese" model is applicable in all cases, either in case of high-tenacity fibres or in case of standard Nylon 6 textile fibers. Although the 3-phase X-ray analysis is now routinely performed, the basic issue of 2-phase *vs.* 3-phase model has not yet been resolved.

We have investigated the suitability of both models and found out that the 3-phase model which is suitable for high-tenacity Nylon 6 fibres cannot be applied in case of aliphatic Nylon 6 fibres manufactured by standard melt spun process. The microfibrillar structure of these fibers resembles to the microfibrillar model of PE more than to the morphology of high-tenacity Nylon 6 fibres. The generally established opinion about applicability of the 3-phase model for all aliphatic Nylon 6 fibres, regardless of the fiber forming process, is not acceptable. The key finding is, however, that Nylon 6 fibers can exist, depending on the forming process, in two morphologically different modifications corresponding to the above-mentioned models. By altering the fiber forming process it is possible to alter the morphology and to control the distribution of amorphous extended interfibrillar and intrafibrillar molecules, and to widen the range of mechanical and thermal properties.

Keywords: Nylon 6; 2-phase microfibrillar model; 3-phase microfibrillar model; morphology; microfibril; supermolecular structure

*Corresponding author.

1. INTRODUCTION

It is well known that the properties of semi-crystalline polymers depend on their morphology and that the morphological structure can be successfully modified and controlled by heat, stress and other variables during the fiber forming process. The effect of morphological modifications on properties is particularly pronounced with semi-crystalline fibers where the structural modifications lead to distinctive differences in tensile strength and modulus (*e.g.*, high-tenacity and standard Nylon 6 fibers). Since it is highly important to understand the interdependence of structure and properties, from both academical and technological view point, it is not surprising that so many studies have been made in this field [1]. They have revealed important and applicable dependences between the fibers properties (tenacity, modulus *etc.*) and their different structures which results by drawing, tempering *etc.* Regardless of the applicable empirical dependence, the effect of morphology on fibers properties has not been quantitatively defined yet despite of relatively good qualitative knowledge of morphology. Not only that the structure of semi-crystalline oriented fibers is complex due to the nature of their origin, but there are also lots of other problems, such as different interpretations of various structural models, that make a quantitative estimation of these structures still more difficult and complicated.

In scientific literature the microfibrillar structure of various aliphatic Nylon 6 fibers has been consistently presented by a modification of the microfibrillar model, the so-called "Swiss-cheese" model [2] which has been criticized by the author [3] of the microfibrillar model. The widely spread opinion is that the 3-phase "Swiss-cheese" model is applicable in all cases, either in case of high-tenacity Nylon 6 fibers or in case of standard Nylon 6 textile fibers manufactured by standard melt-spun process. Although different interpretations of the microfibrillar structure by two authors stirred up polemics in technical literature they have not incited any significant investigations in that direction. The "Swiss-cheese" model has been adopted as a model of microfibrillar structure of all aliphatic Nylon 6 fibers, partly also owing to the only one visual graphical interpretation of the Nylon 6 fibers microfibrillar structure.

Since some results of our researches (*e.g.*, change in the small-angle X-ray scattering (SAXS) intensity, decrease in intensity and disap-

pearance of SAXS at high draw ratios, reduced diameters of microfibrils, crystallites length to diameter ratio, more-than-linear modulus increment, pseudoaffine deformation of microfibrillar structure, a highly anisotropic fibrillar morphology) were not in accordance with the predictions of the above-mentioned model we have investigated whether the "Swiss-cheese" model that is suitable for high-tenacity Nylon 6 fibers is applicable also in case of the microfibrillar structure of textile Nylon 6 fibers formed by standard melt-spun process.

We have investigated the impact of the Nylon 6 fibers plastic deformation on formation of supermolecular fibrillar structures and their transformation in various circumstances by using experimental methods: wide- and small-angle X-ray scattering WAXS, SAXS, scanning electron microscopy SEM, ion etching, FTIR, pulse propagation, thermo-acoustics, dynamic mechanical spectroscopy, DSC, thermomechanics, polarized fluorescence. It is very interesting from the technology viewpoint to understand how plastic deformation influences the fibers structure since this is the basis for development of fibers with enhanced, better properties. The results of investigation cannot be explained by the established "Swiss-cheese" morphological model for high-tenacity fibers but much better by the microfibrillar model.

The paper starts with the description of the most important properties of both models and their differences and continues by explaining the supermolecular arrangement in standardly melt-spun Nylon 6 fibers by using the microfibrillar model. The experiments have confirmed that the microfibrillar structure of fibers does not depend solely on the polymer chemical composition but on the fiber forming process as well. Nylon 6 fibers can exist, depending on the forming process, in two morphologically different modifications that can be described by both above-mentioned microfibrillar models.

2. TWO MORPHOLOGICAL MODELS AND THEIR DIFFERENCE

In order to estimate the suitability of the two models, the microfibrillar and the "Swiss-cheese" model, for Nylon 6 fibers made by standard melt-spun process it is necessary to know the characteristics of each of them and the key qualitative differences is description and presentation of the supermolecular structure of oriented Nylon 6 fibers.

2.1. The Microfibrillar Model [3]

The microfibrillar model of supermolecular structure is a generally established model used to describe and explain certain properties of oriented fibers and their modifications during mechanical and thermal processing. The major characteristics of the microfibrillar model (Fig. 1) can be summarized as follows:

1. It is two-phase serial microfibrillar model of the supermolecular structure (crystallites and amorphous domains arranged in series).
2. The model is represented by long and thin microfibrils, the basic elements of the supermolecular structure and the carriers of fibers properties. The basic properties of microfibrils are: geometry, two-phase of structural arrangement and anisotropy.
3. Microfibrils originating in stacks of lamellae form small bundles of long and thin fibrils that do not differ substantially either in the crystallites orientation or in the draw ratio.
4. On drawing lamellae in stacks "break" and incorporate into small bundles of microfibrils. By unfolding the macromolecules at the

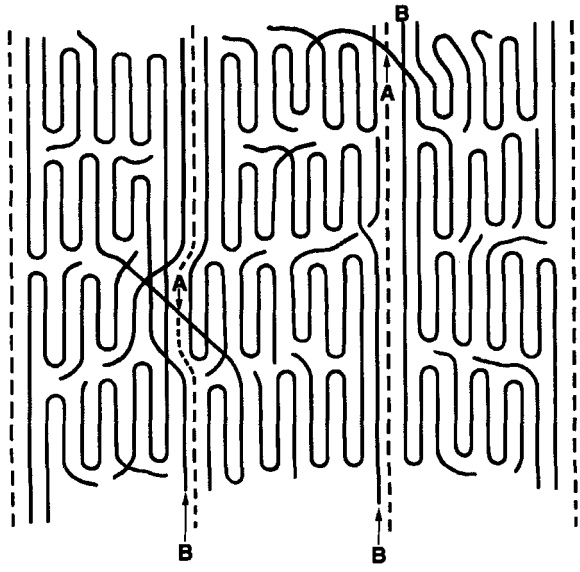

FIGURE 1 Microfibrillar model of the fibre structure [3]; A-interfibrillar, B-intrafibrillar tie molecule.

points of lamellae "breakage" a multiplicity of intramicrofibrillar tie molecules are produced. In accordance with the geometry of formation these tie molecules are mainly located on the outside of microfibrils where they create a layer of almost fully stretched, taut and arranged macromolecules.

5. After drawing switch-board and interlamellar molecules interconnect crystallites in various microfibrils; these are the intermicrofibrillar tie molecules on the boundary layer between adjacent microfibrils.
6. Crystallites inside microfibrils are connected by intramicrofibrillar tie molecules and between microfibrils by intermicrofibrillar tie molecules. The linkage over amorphous domains in fibrillar structure results in a high elastic modulus.
7. Both types of tie molecules (intra and inter) represent more or less amorphous domains and are inhibited at crystallization due to the high ratio of surface to volume and imperfect lateral matching (molecules are embedded in differently oriented crystallites).
8. The transformation into the microfibrillar structure is completed at a relatively low draw ratio between 2 and 3 for Nylon 6 fibers.
9. Further drawing is possible due to plastic deformation of the formed fibrillar structure as a result of axial displacement of fibrils and can be described by the affine deformation of their gravity centers, *i.e.*, with preservation of distances proportion between them.
10. On drawing shear stresses occur on inclined fibrils and cause slipping of microfibrils (this contributes little to the specimen deformation). Both types of deformation (fibrils axial displacement and microfibrils slips) extend interfibrillar tie molecules and increase their volume share that increases approximately linear with the draw ratio.
11. Shear forces acting on microfibrils deform crystallites by causing slips inside crystallites. Segments of crystallites gradually penetrate into amorphous domains. The boundary lines between crystallites and amorphous domain disappear, the coherent length of long period is shorteneded and the electron density between both domains is reduced to the degree at which the SAXS meridian reflection disappears.
12. Slipping of crystallites segments creates quasi-crystalline bridges that interconnect crystallites over amorphous domains and increase

the force transfer elements beside the increase due to the interfibrillar tie molecules orientation. The result is more-than-linear elastic modulus increment with the draw ratio, despite of less-than-linear increment of interfibrillar tie molecules due to their final length. Random slips of crystallites segments inside microfibrils add to the homogeneity of the inside stress distribution.

13. The microfibrillar model takes into consideration three types of plastic deformation: axial displacements of fibrils, intrafibrillar shear displacement of microfibrils and shear displacement of crystallites segments in microfibrils.

2.2. The "Swiss-cheese" Model [2]

The "Swiss-cheese" model (Fig. 2) is an established model used to present the structure and to explain the properties of PA and PES

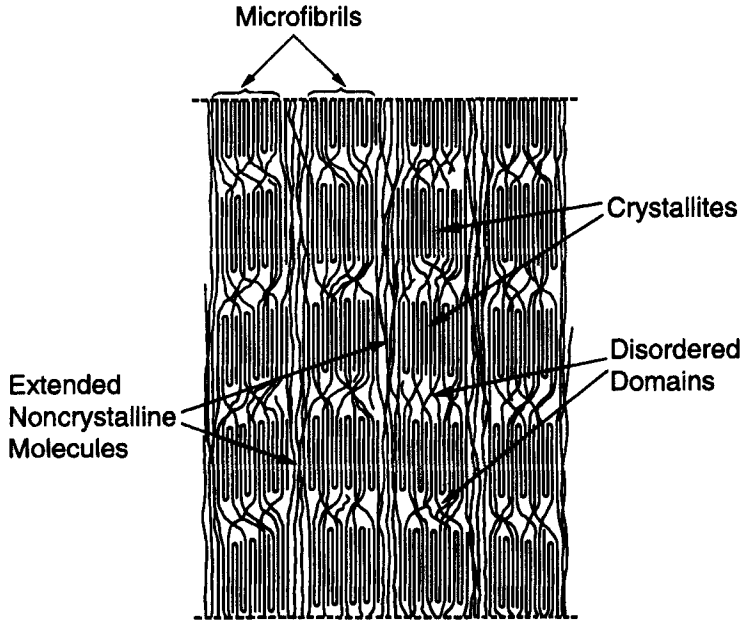

FIGURE 2 Structural model of Nylon 6 fibers ("Swiss-cheese" model) [2].

fibers. Its structural characteristics can be summarized as follows:

1. It is a three-phase serially-parallel microfibrillar model of fibers supermolecular structure (crystallites and amorphous domains arranged in series, and the matrix, *i.e.*, the interfibrillar component of extended taut molecules, parallelly along microfibrils).
2. Main carriers of mechanical properties are interfibrillar taut tie molecules (the third phase).
3. Weak microfibrils with crystallites and amorphous domains arranged in series act as "holes" in a dense matrix, since on drawing the crystallites are getting smaller by unfolding the macromolecules as a rule.
4. Slack tie molecules are distributed more or less uniformly over the cross section of microfibril.
5. The matrix is made up of almost fully extended interfibrillar amorphous tie molecules that can easily crystallize too.
6. A very important drawing mechanism are relative displacements of microfibrils and their thinning and the formation of a dense interfibrillar component of extended molecules (the third phase).
7. The longitudinal structure of microfibril (length of crystallites and amorphous domains, *i.e.*, the long period) remains practically unchanged during drawing and the SAXS meridian reflection does not disappear either at highest draw ratios.
8. Microfibrils are getting considerably thinner than the fiber itself, the distances between microfibrils increase, the strength considerably thinner than the fiber itself, the distances between microfibrils increase, the strength of microfibrils does not change substantially.
9. There is no extending of microfibrils but only their side-by-side shear sliding. The molecules removed from the surface of microfibrils form an interfibrillar component the density of which is similar to the average density of microfibrils. The substantial increase of intefibrillar tie molecules is due to reduction of the microfibrils volume.
10. The model presumes the existence of at least three domains (crystallites, amorphous domains, matrix) of different arrangement and density. The properties of tensile force, modulus,

diffusion and shrinkage force are determined by the matrix. Microfibrils provide dimensional stability.

11. Since the tensile strength is determined by the matrix, *i.e.*, the interfibrillar taut tie molecules and not the microfibrils ("holes"), the model of the cross section of fibres looks like the eyed (microfibrils) Swiss cheese.

The differences between the two microfibrillar models are summarized and highlighted in Table I.

TABLE I Differences between the two models

a) The microfibrillar model	*b) The "Swiss-cheese" model*
• two-phase series model (crystallites, amorphous domains)	• three-phase serially-parallel model (crystallites, amorphous domains, matrix)
• basic carriers of properties are microfibrils	• basic carrier of properties is the oriented matrix, *i.e.*, the extended interfibrillar tie molecules
• intrafibrillar tie molecules are concentrated mainly on the outer boundary of microfibrils	• intrafibrillar slack tie molecules are distributed more or less uniformly inside microfibrils
• smaller portion of interfibrillar tie molecules is distributed between fibrils and microfibrils	• a bigger portion of interfibrillar tie molecules form the oriented matrix (the third phase)
• bundles of microfibrils make up a fibril which is formed by transformation of a complete stack of lamellae	• microfibrils are produced directly in the fiber forming process
• interfibrillar tie molecules originate in switch-board and interlamellae molecules and tie molecules	• interfibrillar tie molecules originate in unfolding of crystallites, *i.e.*, molecules removed from crystallites surface (on account of reduction of microfibrils volume)
• the mass of microfibrils does not change considerably during drawing	• the mass of microfibrils is considerably reduced by drawing, microfibrils are thinning and extended molecules of interfibrillar component (third phase) are produced
• the structure of microfibrils changes on drawing	• the structure of microfibrils remains unchanged on drawing
• the distances between microfibrils decrease on drawing	• the distances between microfibrils increase on drawing
• tensile stress and modulus of microfibrils increase by drawing	• tensile stress and modulus of microfibrils remain unchanged by drawing
• more-than-linear modulus increase on drawing	• modulus linear increase on drawing
• the SAXS meridian reflection disappears at a boundary draw ratio and merges with background	• the SAXS meridian reflection does not disappear either at the highest draw ratios

3. EXPERIMENTAL

3.1. Preparation of Specimens

The undrawn Nylon 6 monofilament yarn Ultralon®, the material used for investigating plastic deformation at various draw ratios, is a product of the Julon factory, the producer of polyamide filaments and granulates from Ljubljana, Slovenia. The polymer was produced by the continuous polymerization process and demonomerized in vacuum and the fibers were produced by spinning from the melt of relative viscosity $\eta_{rel} = 2.57$. The unoriented and semicrystalline monofilament was conditioned at standard conditions and then drawn on a laboratory drawing device with 0.615 m long drawing zone. Drawing up to various draw ratios λ was carried out at the ambient temperature 24°C ± 1°C (four specimens) and at higher temperature. The preheating and plate (0.20 m long) heater temperature were maintained during drawing at 80°C ± 1°C and at 184°C ± 2°C, respectively (seven specimens).

Undrawn monofilament	$\lambda =: 1.00$
Drawn at 24°C ± 1°C	$\lambda =: 1.84, 2.84, 3.90, 4.20$
Drawn at 80°C and at 184°C ± 2°C	$\lambda =: 1.78, 2.77, 3.82, 4.25, 4.62, 5.12, 5.53$

The specimens numbers mean the actual draw ratio stated from the linear density of undrawn to drawn monofilaments.

3.2. Experimental Methods

Experimental methods were selected so that they optimally characterized the morphology, structure, anisotropy as well as relaxation and viscoelastic properties of monofilaments in view of the degree of plastic deformation. Experimental methods encompassed:

- basic experimental methods (linear density, cross-section geometry, tensile tests *etc.*),
- morphology investigation methods (scanning electron microscopy of surface, ionetching, topography and morphology of the inside of fibers and their fractures in liquid nitrogen),
- structure investigation methods (wide-angle X-ray scattering or WAXS, small-angle X-ray scattering or SAXS, DSC, mass density),

- anisotropy measuring method (pluse propagation rate, thermo-acoustics, birefringence, FT-IR spectroscopy, polarized fluorescence),
- relaxation and visco-elasticity experimental methods (shrinkage, creep, stress relaxation, thermo-mechanical spectroscopy, stress-strain diagram analysis Dinara©, dynamic mechanical spectroscopy).

3.2.1. Scanning Electron Microscopy (SEM)

Morphological and topographical changes of surface in the macro-neck zone and the inside of split monofilaments after drawing, was investigated by using a scanning electron microscope JSM-U2 JEOL. The identical method was also used for observing the morphology and topography of etched surfaces and the shapes of monofilaments ruptures during a tensile test. Preparations used for monitoring surfaces, cross-sections, topography and morphology of fibers inside and ruptures were coated by C and Au or by the 90% Au/10% Pd alloy in a 15–20 nm thick layer. The electrons accelerating tension was 10 kV, the angle of inclination of the preparation holder to the microscope optical axis was 45° and the working distance 12 mm at corresponding magnifications.

3.2.2. Wide-Angle X-Ray Scattering (WAXS)

X-ray diffraction patterns were recorded by the Phillips difractometer model 1010 having a texture attachment and a vertical goniometer, by filtering CuK_α radiation through a Ni filter. X-ray scattering took place at the following conditions: Cu cathode, Ni filter, tension 40 kV, power 24 mA, goniometer rate $1° \, min^{-1}$, paper rate $0.5 \, cm/min^{-1}$, collimator: divergence 1°, Geiger-Mueller counter at tension 1.65 kV. All measurements were made in a radiographic symmetrical technique, with a bundle of monofilaments (1 mm) in vertical direction, in the range of angles of inclination 2θ from 12° to 32°. For separation of overlapping crystalline reflections and amorphous component and for the quantitative structural analysis of Nylon 6 the analytical method developed by Heuvel [4] and his collaborators was used. On the basis of statistical analysis of diffraction patterns with distinctly

separated peaks and certain adopted constant values, the computer programme [4] can describe the most diversified diffraction patterns of Nylon 6 (equatorial, meridian, radial, azimuthal). By using the PEARSON VII [5] program the diffraction curves peaks were separated so that the sums of background and 5 Pearson symmetrical curves agreed with the experimental scattering curve.

3.2.3. Small-Angle X-Ray Scattering (SAXS)

Small-angle X-ray diffraction patterns were recorded by the generators KRM-1, 12 VA, 50 kV, 150 mA, with vacuum cameras with point collimation. The distance between two apertures having a diameter of 0.3 mm each was 125 mm and the specimen-film distance was 164 mm for camera No. 1, 175 mm for No. 2, 180 mm for No. 3 and 170 mm for No. 4. The CuK_α radiation was filtered by the Ni filter. The SAXS curves were derived from X-ray diffraction patterns by scanning with microdensitometer (Joyce-Loebl). The SAXS intensity was analyzed by applying the method developed by Cvankin [6].

3.2.4. Pulse Propagation Rate

Pulse (frequency 10 kHz) propagation rate along Nylon 6 monofilaments was measured by the pulse detector Morgan Dynamic Modulus Tester, Pulse Propagation Meter PPm-5R, (H.Morgan Comp., USA). The specimen of Nylon 6 filament was clamped on one end and stretched over two ceramic piezoelectrical detectors (transmitter and receiver). The stress on monofilaments under test was identical to 500 m mass of monofilament. 50 measurements were made for each specimen.

3.2.5. IR-spectroscopy

Specimens were prepared by paralleling monofilaments in one, approximately 0.8 cm wide and 3 cm long layer and by glueing them together on both ends with adhesive tape. Such single layer of fibers was carefully inserted under low stress, between two metal plates having two symmetrical cutouts. The holder with fibers was inserted in the measuring cell of the IR-spectrometer UR-20 (Carl Zeis, Jena);

the IR-spectra were recorded at wave numbers from $700\,cm^{-1}$ to $1900\,cm^{-1}$ by using the technique with NaCl. The spectra were recorded in a polarized light with the polarized light electrical vector oscillating perpendicular and parallel to the fibers axis and in a general absorption spectrum without polarization.

3.2.6. Polarized Fluorescence

The intensity of polarized fluorescence on a single layer of Nylon 6 fibers of different draw ratios was measured by an universal polarization fluorometer type FOM-1 Jasco (Japan Spectroscopic Co., Ltd.) and registered in polar coordinates from 0° to 360°. Fluorescent molecules Whitex RP were inserted from water solution into the amorphous domains of Nylon 6 monofilaments by the diffusion method. The amount of luminophore in fibers did not exceed 0.05%. The single layer of filaments was positioned on the goniometer desk so that in the same plane lied two polarization vectors of induced and fluorescented light that can be rotated around the normal to plane. The intensity of fluorescented light was registered as a function of the angle between the induced light polarization vector and the fibers axis. Specimens were illuminated on goniometer by the high-pressure mercury lamp inducing light, wave length $\lambda = 365\,nm$. The intensity of fluorescence was registered, through an interference filter with maximum at $\lambda = 435\,nm$, by a photomultiplier and a polar coordinate plotter.

4. RESULTS AND DISCUSSION

The validity of the hypothesis that the "Swiss-cheese" model which is applicable for high-tenacity Nylon 6 fibers is suitable also for the microfibrillar structure of textile Nylon 6 fibers formed by standard melt spun process was investigated by various structural and morphological experiments, measurements of anisotropy and observation of visco-elasticity and relaxation properties; the obtained results were compared with the properties and predictions of both morphological models.

The undrawn monofilament under investigation is a semicrystalline monofilament, composed of lamellae, stacks of lamellae and partly spherulites and of amorphous molecular segments that have not succeeded in crystallizing due to thermo-dynamic conditions (increased changes of conformation entropy). The ratio of amorphous to crystalline structure determined from the WAXS recordings is 80:20. The proofs of such initial crystalline structure are the shapes of SAXS reflections of undrawn and slightly drawn monofilaments.

Drawing provokes the transformation of the initial structure into a microfibrillar structure. This is evidenced by the change of SAXS meridian reflections from circular, point-droplike into four-point and streaky ones (Fig. 3) as well as by the supermolecular morphology seen in the SEM photographs of the inside of split monofilaments (Fig. 4) or in liquid nitrogen broken Nylon 6 monofilaments (Fig. 5). Transformation and formation of microfibrils is more or less completed in the range of draw ratios $\lambda = 2-3$ which is in perfect accordance with the measured mechanical properties (*e.g.*, modulus) that rapidly increase from this draw ratio on and with the predictions of the microfibrillar model.

Although higher draw ratios do not change the image of the supermolecular morphology (SEM) as drastically as the initial stages

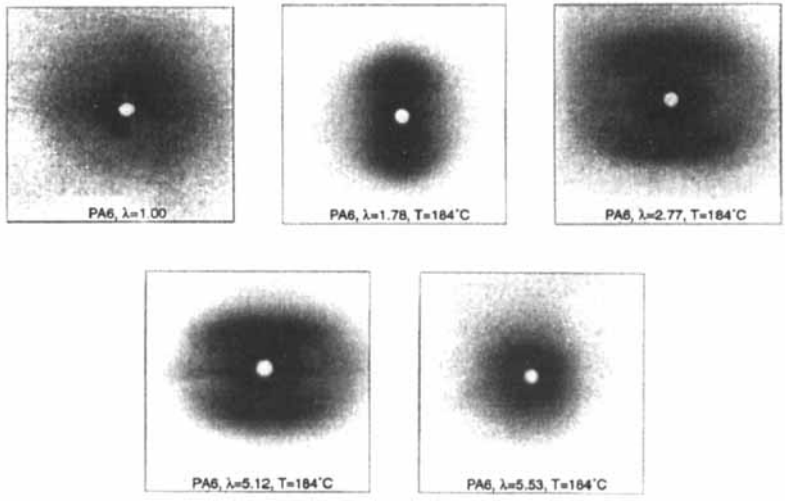

FIGURE 3 SAXS patterns of Nylon 6 fibers with different draw ratio.

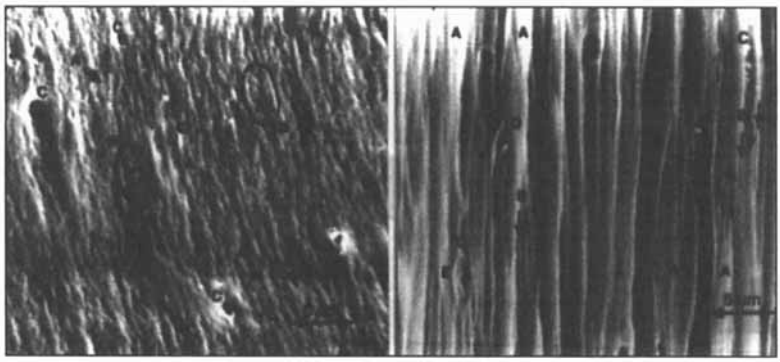

FIGURE 4 SEM photographs of undrawn and drawn $\lambda = 2.84$ Nylon 6 monofilament.

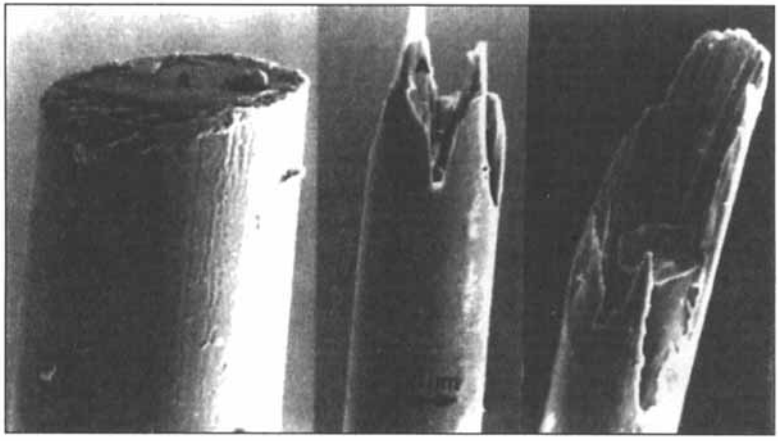

FIGURE 5 SEM photographs of tensile break of undrawn and drawn $\lambda = 2.84$ Nylon 6 monofilaments.

of drawing, they have, however, the impact on microfibrillar structure (SAXS) that continues to change up to the highest draw ratios. In Figure 6 the structural amounts of microfibrils for both draw temperatures are compared. The scheme illustrates four microfibrils at different draw ratios as "playing geometry on paper" but in a scale and by considering the mean orientation angle of crystallites and interfibrillar amorphous share.

On the basis of linear geometry that is not an authentic image of a substance spatial rearrangement at all but admits, anyway, an

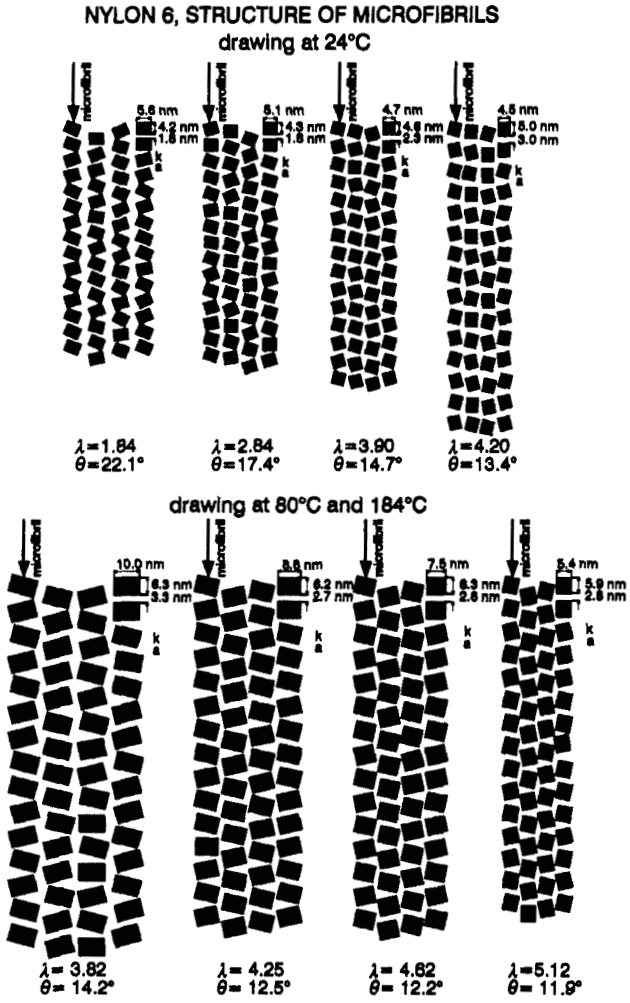

FIGURE 6 Scheme of Nylon 6 microfibrillar structure (λ draw ratio, θ orientation angle of molecules).

approximate notion about the microfibrillar structure development, we can summarize some key findings.

At both draw temperatures microfibrils are formed from the output unoriented monofilament having the structure of stacks of lamellae; they are getting thinner with draw ratio, but their diameter is, however, at higher draw temperature bigger than at lower temperature

(Fig. 6). The fact is that irrespective of draw temperature microfibrils are getting thinner and the length of crystallites and long period increases. The results of experiments show that drawing of microfibrils is important also in the last stage of orientation drawing.

The difference in size of crystallites at both draw temperatures is also very important. At higher draw temperature crystallites are, due to additional crystallization, always bigger than at the ambient temperature. Only very high draw ratios give the crystallites similar by size to those formed by drawing at the ambient temperature because of the shorter time of exposure to high temperature. Higher is the draw ratio, smaller are the crystallites. This is a thermo-dynamic law that also applies to high-speed fiber spinning where crystallites do not have enough time to grow [7].

Changing of the crystallites size in microfibrils with draw ratio λ is illustrated by the crystallites aspect ratio, *i.e.*, the ratio of crystallite length l_c to width D (Fig. 7). The aspect ratio depends upon the draw temperature. Drawing at the ambient temperature gives for identical draw ratios higher crystallites aspect ratios than drawing at higher temperature because of subsequent crystallization and increased width of crystallites. The crystallites aspect ratio in microfibrils increases with draw ratio at both draw temperatures achieving approximately

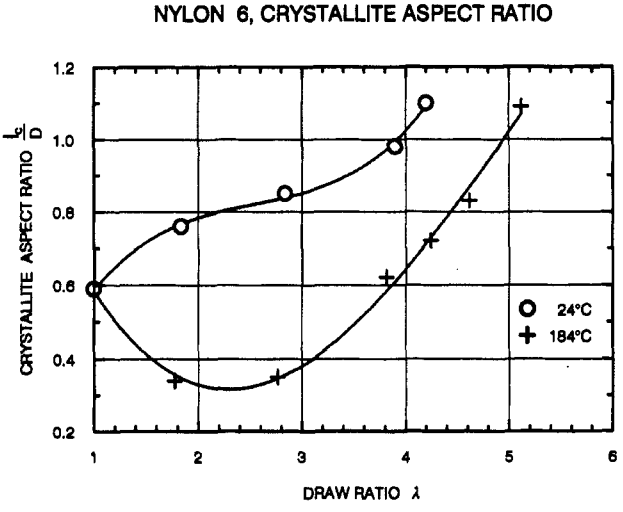

FIGURE 7 Ratio of crystallite length l_c to width D in dependence of draw ratio λ.

1 for boundary λ values. Experiments show that monofilaments have the highest value of tensile stress and modul at the crystallites aspect ratio of 1.1.

Despite of the fact that high draw ratios give similar microfibrillar structure at both draw temperatures, quantitative differences resulting from different draw temperatures remain and hence also the differences in properties. Drawing at higher temperature (compared to drawing at the ambient temperature) provides longer long period, longer crystallites that occupy up to 70% (62%) of long period, higher linear crystallinity 0.70 (0.65) of microfibrils, at similar draw ratios wider microfibrils 8.6 nm (4.5 nm) and longer coherence length of long period 18.6 nm (13.7 nm). The difference in coherence length reflecting a sharper periodicity in crystalline dimensions along the microfibrils in monofilament drawing at higher temperature than in monofilament drawing at the ambient temperature.

The elasticity modulus of drawn microfibrillar structure increases with relative draw ratio of microfibrils $\lambda_f = \lambda/\lambda^*$ more than linearly (Fig. 8) (λ^* is the draw ratio at which the transformation into microfibrillar structure is completed). The relative draw ratio of fibrillar structure at the monofilaments rupture is $\lambda_p^* = 2$, which means

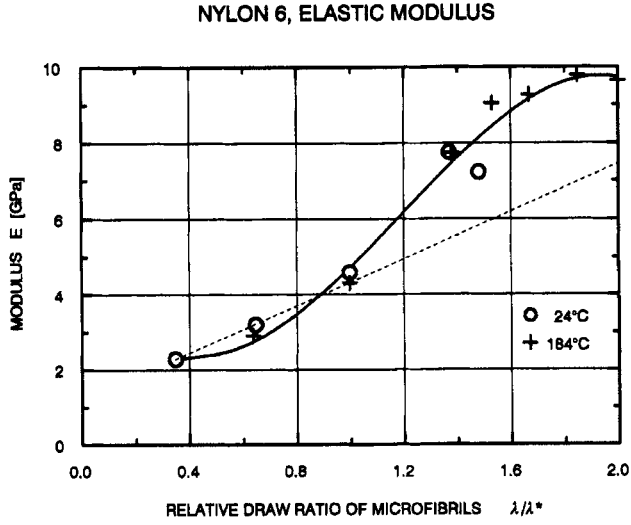

FIGURE 8 Nonlinear dependence of modulus E on relative draw ratio of microfibrils λ_f.

that the deformation of the formed microfibrillar structure up to rupture is relatively small (for 100%) in view of the entire fiber. Therefore, the deformation of fiber is much bigger than the deformation of microfibrils, which is in accordance with the microfibrillar model. The relative draw ratio of microfibrils at rupture ($\lambda_p^* = 2$) does not exceed the draw ratio of fibers as is required by the "Swiss-cheese" model for the formation of extended interfibrillar molecules. The stated share of interfibrillar amorphous domains from 26% to 38% is probably a sufficient stock of molecules that can be extended and can form together with blocks of molecules pulled out of crystallites an interfibrillar, more or less oriented matrix which would correspond to the third component in the "Swiss-cheese" model.

After formation the microfibrillar structure deforms in accordance with the pseudo-affine deformation (Fig. 9) which is characteristic for plastic deformation of semicrystalline polymers. Figure 9 shows the Nylon 6 amorphous domains orientation in coordinates of the second and fourth order orientation factors F_2 and F_4 together with model distribution of orientations [8]. Point $N(0,0)$ represents an ideally isotropic and $(1,1)$ an ideally anisotropic polymer. The

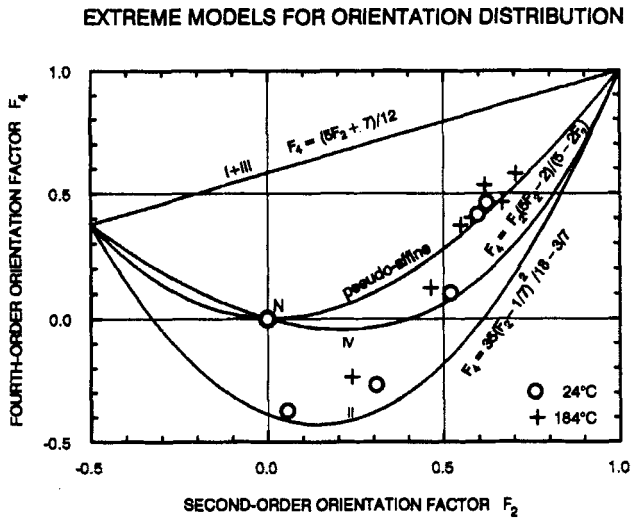

FIGURE 9 Dependence of orientation factors F_4 and F_2 for Nylon 6 with various draw ratios in the model of orientation distributions.

measured orientations of drawn Nylon 6 monofilaments are mainly arranged along the curves of pseudo-affine deformation and model IV. The orientations in specimens with low draw ratio are closer to the distribution II that admits all orientation angles between $0° < \theta < 90°$. The F_4 values for draw ratios $\lambda = 1.00$, $\lambda = 1.84$ and $\lambda = 1.78$ are considerably lower than the values predicted by the pseudo-affine deformation and are the result of the initial state and non-homogenous transformation of substance.

The orientation angles of molecules are within the range admitted by model II. With higher draw ratio the values approach the predicted dependence of orientation function that corresponds to the pseudo-affine deformation model [9] which is also in accordance with the predictions of the microfibrillar model.

The photographs of split Nylon 6 filaments show a distinctly oriented fibrillar structure. Higher is the filaments anisotropy more fringed is the split surface and more distinctive is the fibrillar structure (Fig. 10). This implies that by drawing more and more anisotropic

FIGURE 10 Fibrillar structure of split Nylon 6 fiber.

microfibrils, joined into fibrils and macrofibrils, represent a strong basic element of the fibrous structure, like in microfibrillar model, since they are, by a fiber splitting, torn out of the far less anisotropic surrounding matrix. Due to gradual incorporation of microfibrils into higher morphological units the ends of fibrillar assemblies (microfibrils, fibrils, macrofibrils) always terminate with the tapering ends (Fig. 10). Such picture probably cannot be created only by partly oriented intermicrofibrillar and interfibrillar tie molecules of amorphous domains.

The intensity of the SAXS meridian reflection that corresponds to the repeating arrangement of crystallites and amorphous domains along microfibrils increases with draw ratio up to $\lambda = 3.82$, whilst its width constantly decreases. Higher draw ratios $\lambda = 3.82$ reduce the peak intensity which at $\lambda = 5.53$ completely disappears in the background scattering (Fig. 11) as a result of discontinued periodicity along microfibrils as is predicted by the microfibrillar model.

Such transformation of Nylon 6 monofilaments by drawing corresponds to the predictions of the microfibrillar model. On the basis of experiments and by knowing both models it can be stated that

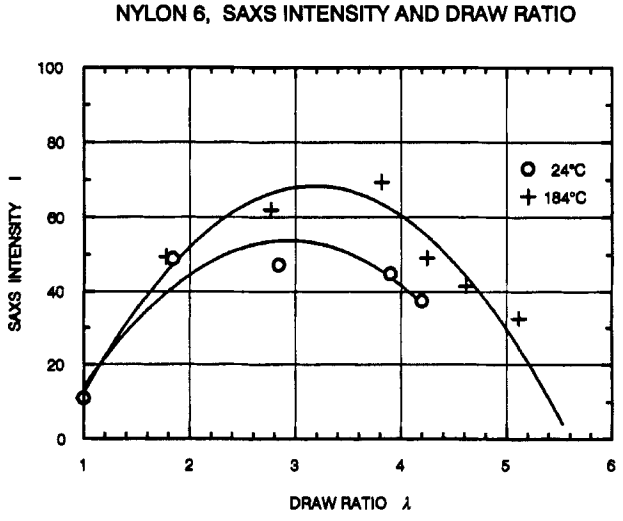

FIGURE 11 SAXS intensity in dependence of draw ratio.

some key experimental results of Nylon 6 transformation, such as:

- nanometric microfibrillar structure,
- crystallites aspect ratio,
- more-than-linear increase of elasticity modulus,
- low relative draw ratio of microfibrillar structure,
- pseudo-affine deformation of fibrillar structure,
- highly anisotropic fibrillar morphology,
- SAXS intensity changes and
- SAXS meridian reflection merging with background at the highest draw ratio

can be explained by the microfibrillar model better than by the "Swiss-cheese" model [10].

Such answer to the hypothesis set forth initially leads to the vital finding that the morphology and hence the properties of Nylon 6 fibers can be altered through modifications of the manufacturing technology. And if it is possible to alter the morphology through technological process, then it is also possible to control the properties of fibers in this way. It seems that the manufacturing process of high-tenacity fibers creates the conditions at which a bigger share of interfibrillar tie molecules form a highly oriented matrix (the third phase), whereas the standard technology creates the morphological structure that suits better to the microfibrillar model. The difference in properties due to different morphology are obvious [11], *i.e.*, high tensile strength (> 1 GPa) and modulus, extreme coherence length (80 nm), high glass transition temperature (99°C), high degree of crystalinity (69%), considerable shrinkage *etc.*

It seems that also in the polymer physics the universality principle does not apply. There is simply no such universal, uniform model that would represent all and would apply to all various morphological structures of fibers composed of flexible molecules. The microfibrillar model is undoubtedly applicable in cases when the microfibrillar structure originates in a stack of lamellae or spherulites and when flexible molecules have enough time for conformational changes. The formation of high-tenacity fibers, however, does not leave enough time to molecules, so the formation of fibrillar morphology is different.

5. CONCLUSION

On the basis of experimental results the hypothesis set forth initially can be converted into the statement that the 3 phase "Swiss-cheese" model that is applicable in case of high-tenacity Nylon 6 fibers does not suit to the microfibrillar structure of textile Nylon 6 fibers formed by standard melt spun process.

By considering the results of our research and the findings about high-tenacity [11, 12] Nylon 6 fibers we can state that:

- the established opinion about suitability of the "Swiss-cheese" model for all aliphatic Nylon 6 fibers, regardless of their forming process, is not acceptable,
- the microfibrillar structure of Nylon 6 fibers made by standard melt spun process is morphologically more similar to the microfibrillar model of PE than to the morphology of high-tenacity Nylon 6 fibers,
- in view of distribution of extended interfibrillar tie molecules across the entire domain of structural elements, *i.e.*, in fibrils and microfibrils of which they are a component part, textile Nylon 6 fibers exhibit more similarity with PE fibers (however with greater share of interfibrillar tie molecules) than with high-tenacity Nylon 6 fibers,
- the microfibrillar structure does not depend only upon a polymer chemical composition but also upon the fiber forming process (Fig. 12),
- control and way of distribution of extended interfibrillar tie molecules are possible only during the fiber forming process and no more during the orientation drawing, hence it follows that,
- modification of fibers orientation drawing does not have any substantial effect on location and way of distribution of interfibrillar tie molecules, which means that it is not possible to drastically modify the microfibrillar structure (*e.g.*, into microfibrillar structure of high-tenacity Nylon 6 fibers) by draw ratio only, but that it is necessary to alter the fiber forming process. It seems that it is easier to modify the morphology of forming fibres than their microfibrillar structure,
- Nylon 6 fibers can exist in two morphologically different modifications, depending on selected fiber forming technology, that can

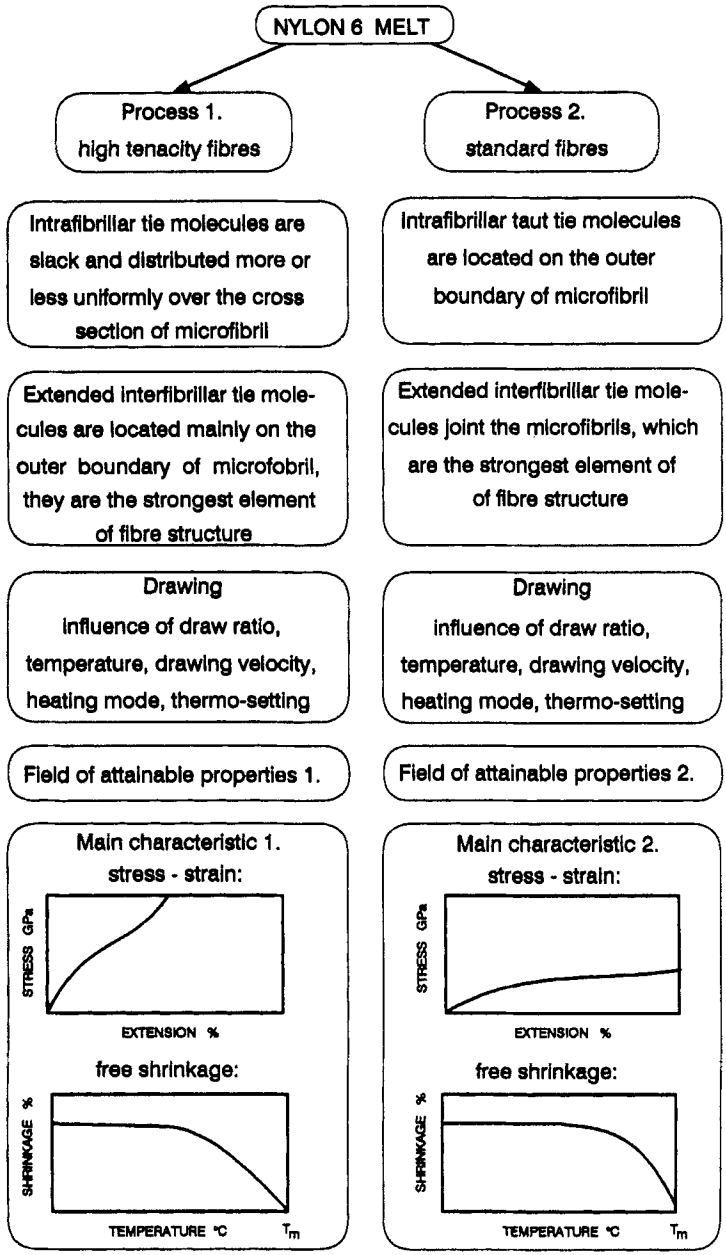

FIGURE 12 Scheme of differences in process and properties between high-tenacity and standard Nylon 6 fibers.

be described by both models, *i.e.*, the microfibrillar model and the "Swiss-cheese" model,

- The 3 phase "Swiss-cheese" model is applicable only in case of high-tenacity Nylon 6 fibers and not for all aliphatic polyamide fibers as has been widely believed so far,
- The researches carried out on Nylon 6 fibers confirm that it is possible to control the distribution of amorphous extended interfibrillar molecules by selecting the fiber forming process and to widen the range of mechanical and thermal properties by enlarging achievable morphological structures; this enables quite a new approach to the development of Nylon 6 fibers with optimal properties for special end-uses.

References

[1] Harisson, P. W. (1970). Fibre Structure, *Textile Progress*, **2**(4); Meredith, R. (1975). The Structure and Properties of Fibres, *Textile Progress*, **7**(4); Mukhopadhyay, S. K. (1989). The Structure and Properties of Typical melt-spun Fibres, *Textile Progress*, **18**(4).

[2] Prevoršek, D. C., Harget, P. J., Sharma, R. K. and Reimschuessel, A. C. (1973). *J. Macromol. Sci. Phys.*, **B8**, 127–156.

[3] Peterlin, A. (1971). *J. Material Sci.*, **8**, 490–508; Peterlin, A. (1975). *Colloid and Polymer Sci.*, **253**, 809–823; Peterlin, A. (1977). *J. Appl. Physics*, **48**, 4099–4108.

[4] Heuvel, H. M., Huisman, R. and Lind, K. C. J. B. (1976). *J. Polym. Sci.-Physics Edition*, **14**, 921–940; Heuvel, H. M. and Huisman, R. (1981). *J. Appl. Polym. Sci.*, **26**, 713–732.

[5] Bukošek, V. (1993). Fitting of the Sum of 5 Pearson VII lines to Nylon 6 WAXS Measurements, Software for Atari and PowerMac, Fortran-77, Ljubljana FNT, TT, p. 67, Adapted for PowerMac from Ref. 4.

[6] Cvankin, D. Ya. (1964). *Vysokomol. Soedin., Ser. A*, **6**, 2078–2082; Cvankin, D. Ya. (1964). *Vysokomol. Soedin., Ser. A*, **6**, 2083–2089; Buchanan, D. R. (1971). *J. Polym. Sci., A-2*, **9**, 645-658.

[7] Ziabicki, A. and Kawai, H. (Ed.) (1985). *High-Speed Fiber Spinning*, J. Wiley & Sons, NY, p. 326.

[8] Nomura, S., Nakamura, N. and Kawai, H. (1971). *J. Polym. Sci., A-2*, **9**, 407–420.

[9] Ward, I. M. (Ed.) (1975). *Structure and Properties of Oriented Polymers*, Applied Sci. Publ. Ltd., London.

[10] Bukošek, V. (1997). Kompleksna analiza molekulske urejenosti in lastnosti PA6 vlaken (Complex Analysis of Molecular Order and the Properties of Nylon 6 Fibres), University of Ljubljana Publish., NTF, p. 351 (in Slovene).

[11] Prevoršek, D. C. (1998). Visokozmogljiva vlakna iz gibkih polimerov: teorija in tehnologija (*High Performance Fibres From Flexible Molecules: Theory and Technology*), University of Ljubljana Publish., NTF, Ljubljana, p. 494 (in Slovene).

[12] Prevoršek, D. C. and Oswald, H. J. (1990). Melt Spinning of PET and Nylon Fibers, in book: Schultz, J. M. and Fakirov, S. (Eds.), *Solid State Behavior of Linear Polyesters and Polyamides*, Prentice Hall, pp. 131–208.